

Protective effect of exogenous hydrogen sulfide on diaphragm muscle fibrosis in streptozotocin-induced diabetic rats

Rui Yang^{1,2} , Qiang Jia² , Yan Li³ and Shomaila Mehmood¹

¹School of Life Sciences, Anhui University, Hefei 230601, China; ²Department of Physiology, Bengbu Medical College, Bengbu 233030, China; ³Clinical College, Bengbu Medical College, Bengbu 233030, China
Corresponding author: Qiang Jia. Email: jiaq12@sina.com

Impact statement

Diabetes mellitus is a group of chronic metabolic disorders, which causes serious damage to a variety of organs, such as the retina, heart, and skeletal muscle. The diaphragm is an important skeletal muscle involved in respiration in mammals. Fibrosis of the diaphragm muscle affects its contractility, which in turn impairs respiratory function. Accumulating evidence suggests that exogenous hydrogen sulfide (H₂S) exhibits anti-fibrotic activity in diabetes mellitus, but whether and how H₂S exerts this anti-fibrotic effect in the diabetic diaphragm remains unclear. The current work for the first time reveals that exogenous H₂S attenuates hyperglycemia-induced fibrosis of the diaphragm muscle and strengthens diaphragmatic biomechanical properties in diabetes mellitus, and the mechanism may involve the alleviation of collagen deposition by suppression of the nucleotide-binding oligomerization domain-like receptor protein (NLRP) 3 inflammasome-mediated inflammatory reaction. Therefore, H₂S supplementation could be used as an efficient targeted therapy against the NLRP3 inflammasome in the diabetic diaphragm.

Abstract

Diabetes mellitus has been shown to impair respiratory function. The diaphragm is an important skeletal muscle involved in respiration. Hydrogen sulfide (H₂S) is one of the three endogenous gas messengers in mammals, which exhibits anti-fibrotic activity in some types of diabetes-related complications. However, whether and how H₂S exerts its anti-fibrotic activity on the diabetic diaphragmatic muscle remains unclear. In this study, we explored the anti-fibrotic activity of exogenous H₂S on the diaphragm using a streptozotocin (STZ)-induced diabetic rat model. The results showed that diaphragmatic biomechanical parameters were decreased, whereas the levels of inflammatory cytokines, collagen, and nucleotide-binding oligomerization domain-like receptor protein (NLRP) 3 inflammasome-related protein expression were increased in diabetic diaphragms. This implies that diabetes causes fibrosis of the diaphragm muscle through activation of NLRP3 inflammasome. After supplementation with exogenous H₂S, the diaphragmatic biomechanical and pathological alterations were ameliorated and activation of NLRP3 inflammasome was inhibited, followed by a decline in diaphragm muscle inflammation and fibrosis. These results demonstrate for the first time that exogenous H₂S effectively attenuates STZ-induced diabetic diaphragm muscle fibrosis, and that the underlying mechanism may be associated with suppression of the NLRP3 inflammasome-mediated inflammatory reaction.

Keywords: Hydrogen sulfide, diabetes mellitus, diaphragm, fibrosis, inflammation, nucleotide-binding oligomerization domain-like receptor protein 3 inflammasome

Experimental Biology and Medicine 2020; 245: 1280–1289. DOI: 10.1177/1535370220931038

Introduction

Diabetes mellitus, accompanied by chronic systemic inflammation, is a group of metabolic disorders characterized by high blood glucose levels due to defects in insulin secretion by pancreatic β cells, insulin insensitivity in peripheral tissues, or both.¹ Sustained hyperglycemia

in diabetes is correlated with long-term injury, dysfunction, and failure of multiple organs, such as the retina, kidney, heart, nerve, and skeletal muscle.^{2,3} Diabetes mellitus has been shown to induce respiratory dysfunction by reducing respiratory muscle endurance and vital capacity.⁴ The diaphragm is an important skeletal muscle involved in respiration in mammals.⁵ A previous study by our group

reported that diaphragmatic contractile function significantly declined in streptozotocin (STZ)-induced diabetic rats, and that the mechanism was correlated with excessive oxidative stress and inflammation in diaphragmatic tissue.⁶ Moreover, the excessive inflammatory reaction in diabetes often causes collagen deposition and muscle fibrosis. Recent evidence shows that deposition of collagen in muscles of diabetic animals was higher than in nondiabetic animals.⁷ Once the extent of fibrosis of the diaphragm aggravates, it will inevitably increase its stiffness, and thus, affect diaphragmatic contractile function. Hence, targeting inflammation may be one of the therapeutic strategies in diabetes-induced diaphragmatic damage.

The innate immune cell sensor nucleotide-binding oligomerization domain-like receptor protein (NLRP) 3 inflammasome is a well-studied multi-protein complex.⁸ The NLRP3 inflammasome complex contains NLRP3 protein, the apoptosis-associated speck-like protein containing a caspase activation and recruitment domain (ASC), and Caspase-1.⁹ Upon activation of NLRP3 protein, procaspase-1 is cleaved to release the bioactive form, Caspase-1, which processes precursor interleukin (IL)-1 β and IL-18 into their active forms, aggravating the inflammatory reaction.¹⁰ Many reports suggest that the NLRP3 inflammasome participates in and promotes inflammatory reactions in diabetes mellitus.^{11,12} In addition, activation of the NLRP3 inflammasome drives many types of tissue fibrosis, such as hepatic fibrosis,¹³ renal fibrosis,¹⁴ pulmonary fibrosis,¹⁵ and cardiac fibrosis.¹⁶ However, whether the NLRP3 inflammasome is involved in diabetes-induced fibrosis of the diaphragm muscle remains unclear.

Hydrogen sulfide (H₂S) is one of the three endogenous gas signaling molecules in mammals that exhibits a variety of pharmacological properties, including anti-inflammatory, anti-oxidative, and anti-apoptotic activities.¹⁷ Jia *et al.* reported that sodium hydrosulfide (NaHS, an exogenous H₂S donor) alleviated myocardial inflammation by suppressing NLRP3 inflammasome activation in STZ-induced diabetic rats.¹⁸ Lu *et al.* demonstrated that exogenous H₂S alleviated peritoneal fibrosis by attenuating the over-generation of proinflammatory cytokines, subsequently reducing the synthesis of transforming growth factor (TGF)- β 1 and the accumulation of extracellular matrix (ECM).¹⁹ However, it remains unclear whether and how H₂S exerts its anti-fibrotic effect on the diaphragm muscle in diabetic rats. Hence, the current study is the first attempt to investigate the anti-fibrotic effect of exogenous H₂S on the diaphragm muscle in diabetic rats and explore the related mechanism, i.e. whether it is associated with suppression of the NLRP3 inflammasome-mediated inflammation.

Materials and methods

Animals

A total of 32 healthy male Sprague-Dawley rats (aged eight weeks with body weight (BW) 200–220 g) were provided by the Experimental Animal Management Center of Bengbu Medical College, Anhui, China. The animals were given

free access to normal rodent diet and tap water and kept in conventional rat facilities with an alternating 12 h light/12 h dark cycle circumstance at a relatively constant temperature of 22–24°C. The animal protocols were approved by the Animal Ethics Committee of Bengbu Medical College and conducted in accordance with ethical standards.

Experimental design

The healthy rats were randomly arranged into four different experimental groups with eight rats in each group: normal control (NC), STZ, STZ + NaHS (SH), and NC + NaHS (NH). Diabetes was induced as per our previously described method.⁶ In brief, all the rats were deprived of food overnight (14 h). Next, the rats allocated to the STZ and SH groups were injected intraperitoneally (i.p.) with 55 mg/kg STZ (Sigma-Aldrich, St. Louis, MO; freshly dissolved in citrate buffer). Rats assigned to the NC and NH groups received an i.p. injection of the same volume of citrate buffer. Seventy-two hours after STZ injection, the blood sample was harvested from the tail vein of 12 h-fasted animals and measured using a portable glucometer (Accu-Chek; Roche). The mice with blood glucose over 16.7 mmol/L were considered diabetic. Four weeks after the establishment of the diabetic model, the rats assigned to the SH and NH groups were injected daily with NaHS (56 μ mol/kg, Sigma-Aldrich; freshly dissolved in sterile saline solution), i.p., for four weeks. Rats assigned to the other groups received daily treatment i.p. of the same volume of sterile saline solution over the same time period.

Detection of fasting blood glucose (FBG) and diaphragmatic biomechanical parameters

After treatment for four weeks, the overnight-fasted rats were weighed and anesthetized with isoflurane. The blood was harvested by cardiac puncture to collect serum and the level of FBG was measured using a glucose assay kit (Jiancheng Bioengineering Institute, Nanjing, China). After the rat was sacrificed, the diaphragm was removed rapidly. Diaphragmatic biomechanical parameters were measured ($n = 8$ /group) using the method we previously described.⁶ In brief, the diaphragm strip was made using the left hemidiaphragm with the central tendon and mounted vertically in an organ bath containing Krebs-Ringer buffer at 37°C. The buffer was equilibrated with 5% carbon dioxide/95% oxygen (pH 7.4) and had the following composition (mmol/L): NaCl 135.0, KCl 5.0, CaCl₂ 2.5, NaH₂PO₄ 1.0, NaHCO₃ 15.0, MgSO₄ 1.0, and glucose 11.0. The strip was linked to the transducer which was connected to a micropositioner and then stimulated with the currents via platinum electrodes. The maximum tetanic tension (P_0), peak twitch tension (P_t), maximal rate of contraction ($+dT/dt_{max}$), and maximal rate of relaxation ($-dT/dt_{max}$) were accessed using the Med-Lab biological recording system (Medease Company, Nanjing, China). After diaphragmatic biomechanical parameters were measured, the diaphragm muscle weight (DW)/BW ratio was calculated.

Histomorphological and ultrastructure assessment

One part of fresh right hemidiaphragm muscle ($n=8$ /group) excluding the tendon area was immersed in a solution of 4% formaldehyde, mounted in paraffin, and then sectioned into 4 μm -thickness slices. The slices were dewaxed, dyed with hematoxylin and eosin (H&E), Masson's trichrome, and Sirius Red reagents (Servicebio Biotechnology Co., Ltd, Wuhan, China), and subsequently analyzed by a light microscope for structural abnormalities and a polarized light microscope for collagen detection. Diaphragmatic blue-stained fibrotic area in Masson's trichrome stained slice was analyzed using Image-Pro Plus (IPP) software. A total of five fields of each slice were chosen randomly and the average was reckoned for analysis.

Fresh right hemidiaphragm muscle ($n=8$ /group) was sectioned into the dimension of 1 mm \times 1 mm \times 1 mm, fixed in a solution of 2.5% glutaraldehyde, and subsequently soaked in a solution of 1% osmium tetroxide. The tissue mounted in Epon812 was sectioned into 70 nm-thickness ultrathin slices. These slices were stained with uranyl acetate and lead citrate and subsequently imaged using a JEM-1230 transmission electron microscope (TEM). The mean number of mitochondria per unit area (55 μm^2) and the mean area of each mitochondrion in each group were analyzed using IPP software as per the above-mentioned method.

Determination of diaphragmatic hydroxyproline content

The content of hydroxyproline in the right hemidiaphragm muscle ($n=8$ /group) was measured using a hydroxyproline assay kit (Jiancheng Bioengineering Institute). Briefly, the diaphragm muscle of each rat was ground with liquid nitrogen and then added into 1 mL of 6 mol/L hydrochloric acid. Following the pH was adjusted to 6.4, activated carbon was added into the diluted hydrolyzation products. After the samples were centrifuged, the supernatant fluids were harvested and incubated with the detection solution for 15 min at 60°C. The optical density value of each sample was determined using a spectrophotometer at a wavelength of 550 nm. The content of hydroxyproline was calculated using the formula according to the manufacturer's instruction.

Quantitative real-time polymerase chain reaction analysis

Total RNA in the left hemidiaphragm muscle ($n=8$ /group) was isolated on ice using a TRIzol reagent (Invitrogen, Waltham, MA). An equal amount of total RNA was reverse transcribed to cDNA in accordance with the protocol of the PrimeScript real time reagent kit (Takara Biotechnology, Dalian, China). The primer sequences of target genes including collagen-I, collagen-III, TGF- β 1, and β -actin were detailed in Table 1. Target genes were amplified and quantified using SYBR Premix Ex Taq II (Takara Biotechnology). The relative gene expression was analyzed

Table 1. Primers used in this study.

Gene	Primer sequence	Length (bp)
TGF- β 1	Forward: 5'-CCAAGGAGACGGAATACAGG-3' Reverse: 5'-ATGAGGAGCAGGAAGGGTC-3'	156
Collagen-I	Forward: 5'-GAGAGAGCATGACCGATGGA-3' Reverse: 5'-CGTGCTGTAGGTGAATCGAC-3'	251
Collagen-III	Forward: 5'-GGCTGCACTAAACACACTGG-3' Reverse: 5'-TGTTGACGAGATTAAGCAAG-3'	229
β -Actin	Forward: 5'-CGTAAAGACCTCTATGCCAACA-3' Reverse: 5'-AGCCACCAATCCACACAGAG-3'	163

using the $2^{-\Delta\Delta\text{Ct}}$ method and standardized against the housekeeping gene β -actin.

Determination of diaphragmatic inflammatory cytokines

Part of right hemidiaphragm muscle ($n=8$ /group) was ground with liquid nitrogen and homogenized in a nine-fold volume of ice-cold saline solution. After centrifugation, the supernatant fluids were collected to determine the protein concentrations using a bicinchoninic acid protein assay kit (Jiancheng Bioengineering Institute). Next, the levels of IL-1 β , IL-6, IL-18, and tumor necrosis factor (TNF)- α were measured using corresponding commercially enzyme-linked immunosorbent assay kits (Elabscience Biotechnology, Wuhan, China), as per the manufacturer's instructions.

Western blot assessment

Part of left hemidiaphragm muscle ($n=8$ /group) ground with liquid nitrogen was homogenized on ice using the radioimmunoprecipitation assay lysis buffer with phenylmethanesulfonyl fluoride (Beyotime Biotechnology, Shanghai, China). After centrifugation, the protein-containing supernatant was harvested to determine the protein concentration. Equal amounts of protein were loaded onto 12% SDS-PAGE and thereafter transferred onto PVDF membranes. After immersing with 5% skim milk powder in tris-buffered saline Tween-20, all the membranes were probed overnight with primary antibodies directly against ASC (Santa Cruz Biotechnology, CA), NLRP3 (Boster Biological Technology, Wuhan, China), Caspase-1 (p20; Boster Biological Technology), and β -actin (Proteintech Biological Technology, Wuhan, China) at 4°C. Subsequently, membranes were incubated with the corresponding horseradish peroxidase-conjugated IgG secondary antibodies (Boster Biological Technology). The protein bands were visualized with enhanced chemiluminescence detection reagents (Servicebio Biotechnology Co., Ltd) and imaged with a ChemiDoc XRS system. The band density was determined with Quantity One software.

Statistical analysis

Data were expressed as the mean \pm standard deviation (SD). Statistical analysis was conducted by a one-way analysis of variance followed by the Newman-Keuls test.

$P < 0.05$ was considered to suggest a statistically significant difference.

Results

Effects of H₂S on FBG, DW, BW, and DW/BW

After different treatment for four weeks, the results showed that compared with the normal rats, the level of FBG was notably elevated, whereas the levels of DW, BW, and DW/BW were reduced in the diabetic rats. Compared with the STZ group, although FBG was unaffected by exogenous H₂S, the levels of DW, BW, and DW/BW were elevated in the SH group. There were no statistical differences between the NC and NH groups (Figure 1).

Effects of H₂S on diaphragmatic biomechanical parameters

As shown in Figure 2, in contrast to the NC group, P_0 , P_t , $+dT/dt_{max}$, and $-dT/dt_{max}$ were evidently reduced in the STZ group. Compared with the STZ group, P_0 , P_t , $+dT/dt_{max}$, and $-dT/dt_{max}$ were notably elevated in the SH group. There were no statistically significant differences in diaphragmatic biomechanical parameters between the NC and NH groups. The results indicated that exogenous H₂S effectively improved the tested biomechanical properties of the diaphragm muscle fibers in diabetic rats.

Effects of H₂S on diaphragmatic histological and ultrastructural changes

H&E staining showed that the cross-sectional shape of the diaphragm muscle fibers of the normal rat was regular, the

nuclei were distributed on the edge of the muscle cells, and inflammatory cells were rare. In the STZ group, the muscle fiber cross-section was irregular and the notable infiltration of inflammatory cells was elevated compared with the normal diaphragm. After supplementation with exogenous H₂S, diaphragmatic damage was markedly ameliorated and infiltration of inflammatory cells was apparently reduced in the SH group. There were no obvious pathological alterations between the NH and NC groups (Figure 3(a)).

The ultrastructure of the diaphragm muscle in the NC group showed that the muscle sarcomeres were arranged in a neat way with clear Z lines and were of even length. In the STZ group, the myofilaments were partly ruptured, the sarcomere was disordered, and the mitochondria were swollen. Supplementation with exogenous H₂S evidently ameliorated diaphragmatic injury in the SH group (Figure 3(b)). As shown in Figure 3(c) and (d), compared with the NC group, the number of diaphragmatic mitochondria was reduced, whereas the area of each mitochondrion was increased in the STZ group. H₂S treatment evidently improved the above indexes in the SH group. These findings suggested that exogenous H₂S exhibited protective properties in STZ-induced diaphragmatic injury.

Effects of H₂S on diaphragm muscle fibrosis

In Masson's trichrome staining, the diaphragmatic collagen fibers of the rat were stained blue (Figure 4(a)). In Sirius Red staining, the diaphragmatic collagen fibers were stained red under light microscopy (Figure 4(b)); the collagen-I was stained red and the collagen-III was stained green under a polarized light microscope (Figure 4(c)).

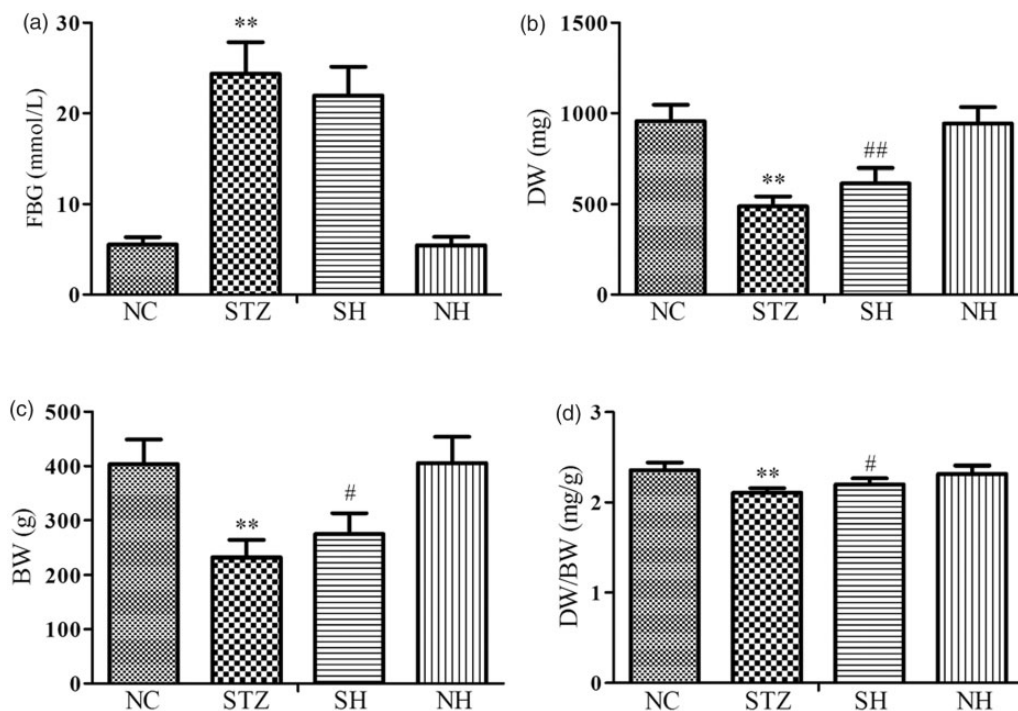


Figure 1. Effects of H₂S on (a) FBG, (b) DW, (c) BW, and (d) DW/BW in the different groups. Values, mean \pm SD; $n = 8$; * $P < 0.01$ vs. NC group; # $P < 0.05$, ## $P < 0.01$ vs. STZ group; NC: normal control group; STZ: streptozotocin group; SH: STZ + sodium hydrosulfide group; NH: NC + sodium hydrosulfide group.

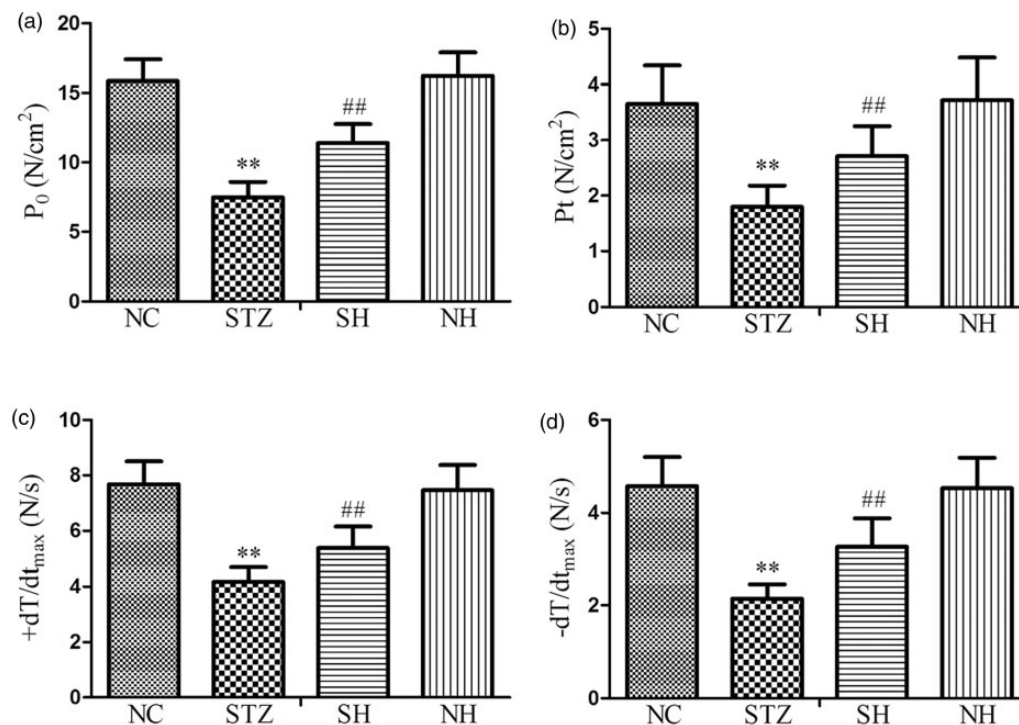


Figure 2. The levels of (a) P_0 , (b) P_t , (c) $+dT/dt_{max}$, and (d) $-dT/dt_{max}$ in the different groups. Values, mean \pm SD; $n = 8$; ** $P < 0.01$ vs. NC group; ## $P < 0.01$ vs. STZ group; NC: normal control group; STZ: streptozotocin group; SH: STZ + sodium hydrosulfide group; NH: NC + sodium hydrosulfide group.

The results showed that diabetes caused severe collagen fibers deposition in the diaphragm muscle. H_2S supplementation notably reduced the extent of collagen fibers deposition in the diabetic diaphragm. There were no obvious histological differences between the NC and NH groups.

Quantitative analysis of Masson's trichrome staining (Figure 4(d)) and the hydroxyproline content (Figure 4(e)) revealed significant rises in collagen formation and deposition in the STZ group in contrast to the NC group. Compared with the STZ group, exogenous H_2S noticeably reduced the diaphragmatic collagen formation and deposition in the SH group. The results indicated that exogenous H_2S was able to alleviate fibrosis of the diaphragm muscle in diabetic rats.

Effect of H_2S on the collagens and TGF- $\beta 1$ expression in the diaphragm

As shown in Figure 5, the mRNA expression levels of collagen-I, collagen-III, and TGF- $\beta 1$ were notably raised in the STZ group compared with the NC group. In contrast to the STZ group, the mRNA expression levels of collagen-I, collagen-III, and TGF- $\beta 1$ were evidently reduced in the SH group, which suggested that exogenous H_2S effectively down-regulated the over-production of collagen through inhibition of TGF- $\beta 1$ signaling in the diaphragm.

Effects of H_2S on diaphragmatic inflammatory cytokines

To investigate the impact of H_2S on the inflammatory response, the concentrations of the proinflammatory cytokines were detected. The results showed that the levels of diaphragmatic proinflammatory cytokines (IL-1 β , IL-6, IL-18, and TNF- α) were notably elevated in the STZ group compared with the NC group. After supplementation with exogenous H_2S , the levels of diaphragmatic proinflammatory cytokines were distinctly reduced in the SH group compared with the STZ group. There were no statistically remarkable differences between the NC and NH groups (Figure 6). The results revealed that exogenous H_2S reduced the over-generation of proinflammatory cytokines in the diabetic diaphragm.

Effect of H_2S on the NLRP3 inflammasome complex in the diaphragm

Compared with the normal diaphragm, the protein expression levels of NLRP3, ASC, and activated Caspase-1 were notably elevated in the diabetic diaphragm. In contrast to the STZ group, exogenous H_2S effectively decreased the expression levels of the NLRP3 inflammasome-related proteins in the SH group, which suggested that exogenous H_2S suppressed the activation of NLRP3 inflammasome (Figure 7).

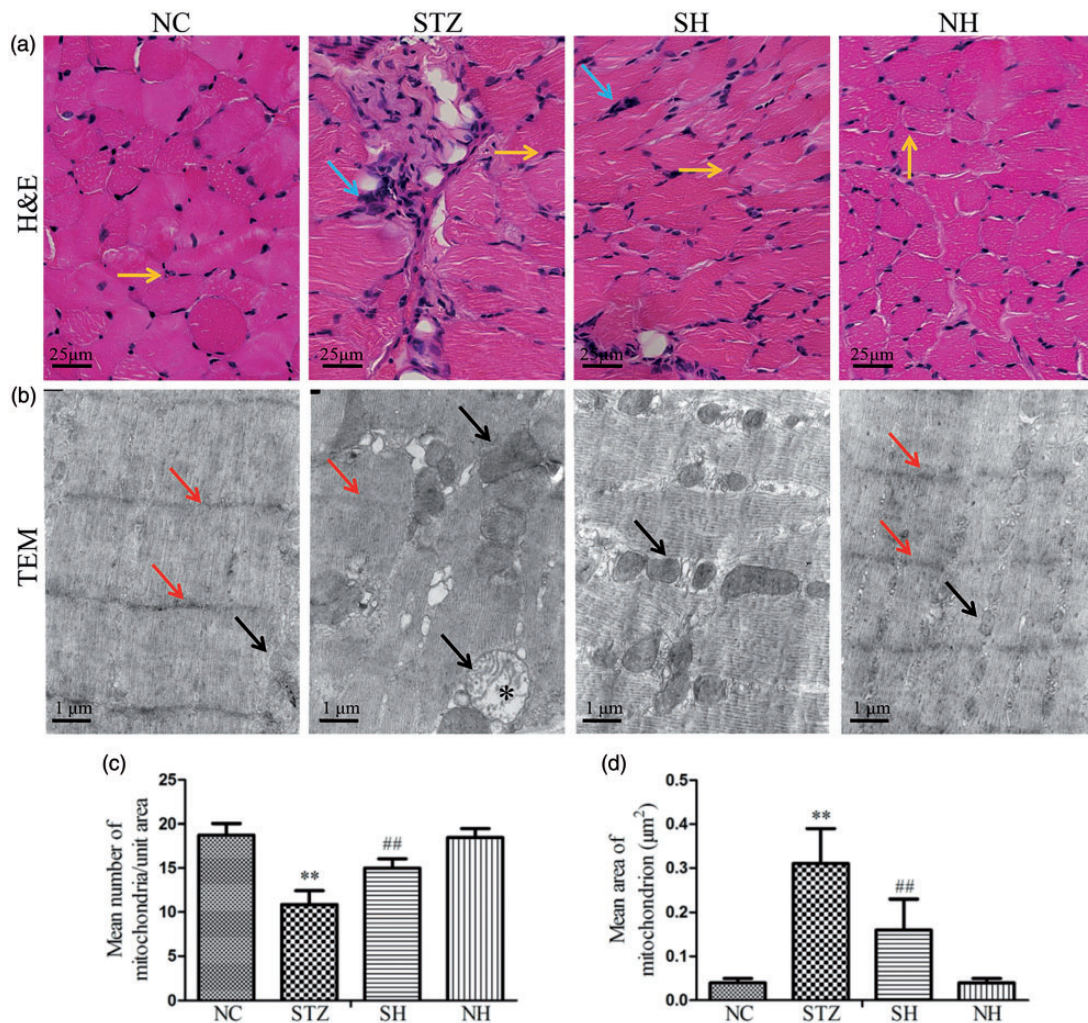


Figure 3. Effects of H₂S on pathological alterations in the diaphragm muscle of the different groups. (a) Representative H&E staining. Yellow arrows refer to the nuclei of diaphragm muscle cells and blue arrows refer to the infiltration of inflammatory cells. (b) Representative ultrastructural alteration. TEM: transmission electron microscope. Red arrows refer to the Z lines and black arrows refer to the mitochondria. Black asterisk refers to the swollen mitochondria. (c) Mean number of mitochondria per unit area. (d) Mean area of each mitochondrion. Values, mean ± SD; $n = 8$; ** $P < 0.01$ vs. NC group; ## $P < 0.01$ vs. STZ group; NC: normal control group; STZ: streptozotocin group; SH: STZ + sodium hydrosulfide group; NH: NC + sodium hydrosulfide group. (A color version of this figure is available in the online journal.)

Discussion

Diabetes mellitus is a group of complicated metabolic disorders, which commonly causes a variety of serious complications, such as diabetic retinopathy, diabetic nephropathy, and diabetic cardiovascular disease.² Increasing evidence has shown that the strength of respiratory muscles is decreased and their endurance is impaired in diabetes mellitus.²⁰ The diaphragm is the most important respiratory muscle *in vivo*, and ventilation insufficiency caused by diaphragmatic dysfunction is the main cause of mortality in some diseases.²¹ The current study shows that diaphragmatic biomechanical parameters and DW/BW ratio were notably reduced; the histomorphology of the diaphragm muscle indicated that integrity of diaphragm muscle cell was destroyed and infiltration of the diaphragm by inflammatory cells was aggravated in diabetic rats. These results confirm that diabetes causes pathological changes in the diaphragm muscle, leading to diaphragmatic damage.

H₂S is one of the three endogenous gas messengers in mammals, which exhibits several important protective properties in diabetes and diabetes-related complications.²² In this study, the data demonstrate that exogenous H₂S did not damage the normal rat diaphragm. On the contrary, in diabetic rats, exogenous H₂S noticeably alleviated the diaphragmatic pathological changes and improved the DW/BW ratio and biomechanical properties. We, therefore, suggest that exogenous H₂S exhibits protective effects on the diaphragm in diabetic animals.

Inflammation is one of the most important causes of diaphragmatic injury in diabetes mellitus.⁶ Inflammatory cells are over-generated and recruited to regions of the damaged diaphragm, as evidenced by infiltration by inflammatory cells and elevated concentrations of proinflammatory cytokines. Cytokines IL-6, IL-1β, IL-18, and TNF-α are considered as proinflammatory mediators *in vivo*, which aggravate the inflammatory reaction. Subsequently, the aggravated inflammatory reaction further stimulates the

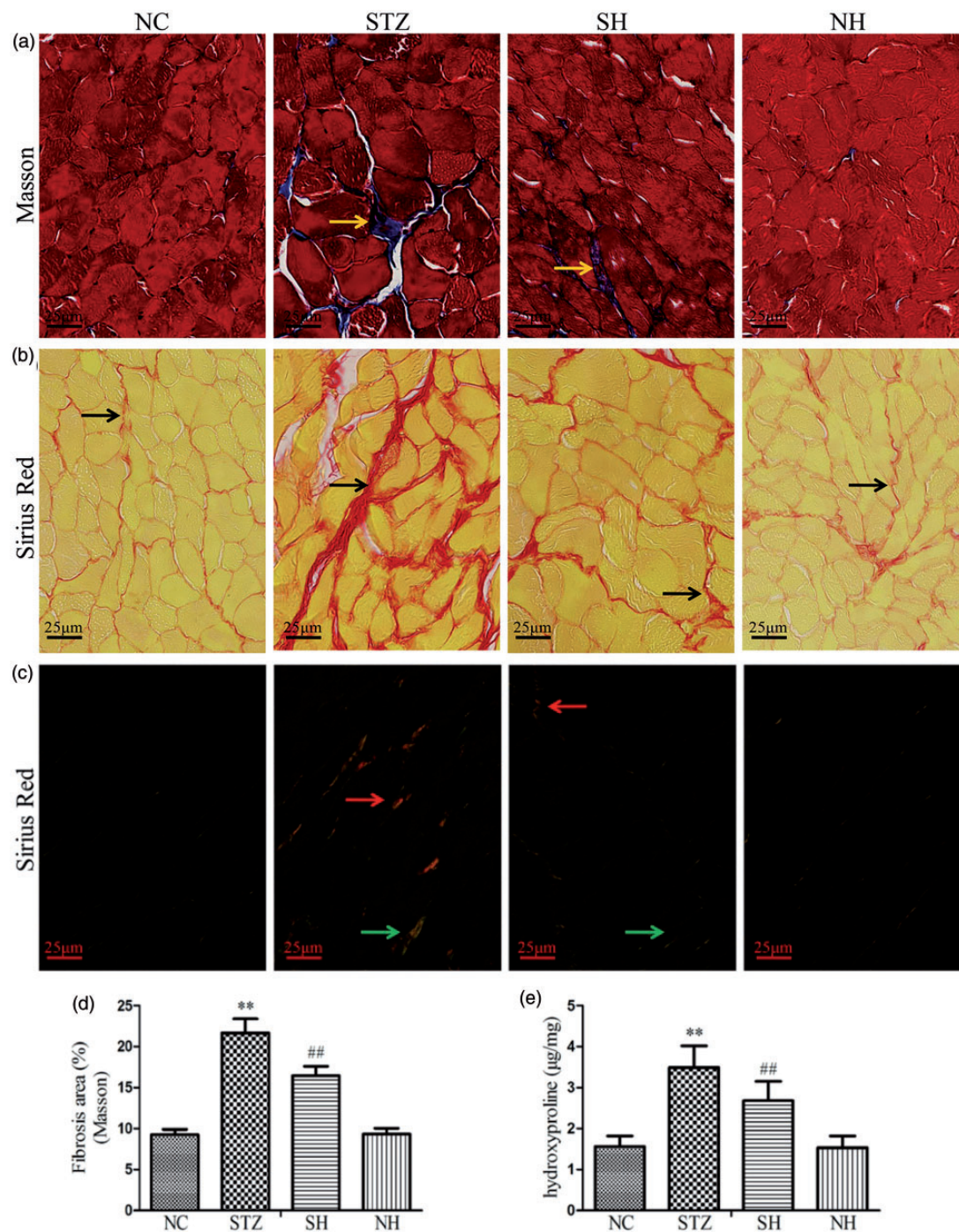


Figure 4. Effects of H₂S on diaphragm muscle fibrosis and hydroxyproline content in the different groups. (a) Masson's trichrome staining under a light microscope. Yellow arrows refer to the blue-stained collagen fibers. (b) Sirius Red staining under a light microscope. Black arrows refer to the red-stained collagen fibers. (c) Sirius Red staining under a polarized light microscope. Red arrows refer to the collagen-I and green arrows refer to the collagen-III. (d) Quantitative analysis for Masson's trichrome staining. (e) Hydroxyproline content was assessed. Values, mean ± SD; n = 8; **P < 0.01 vs. NC group; ##P < 0.01 vs. STZ group; NC: normal control group; STZ: streptozotocin group; SH: STZ + sodium hydrosulfide group; NH: NC + sodium hydrosulfide group. (A color version of this figure is available in the online journal.)

development of fibrotic diseases.²³ Fibrosis is the salient pathological cause of organ dysfunction, which is characterized by continuous generation and excessive deposition of the ECM. In muscle fibrosis, the main components of the ECM are interstitial collagens, including collagen-I and collagen-III. In addition, TGF-β1 is considered as a crucial pro-fibrotic mediator in the fibrotic process.^{24,25} Many

pieces of research have confirmed that TGF-β1 signaling plays a pivotal role in the progression of several fibrotic diseases, such as hepatic fibrosis,²⁶ renal fibrosis,²⁷ cardiac fibrosis,²⁸ and pulmonary fibrosis.²⁹ TGF-β1 signaling directly stimulates generation of ECM and suppresses degradation of collagen. Masson's trichrome staining and Sirius Red staining are commonly utilized to evaluate the

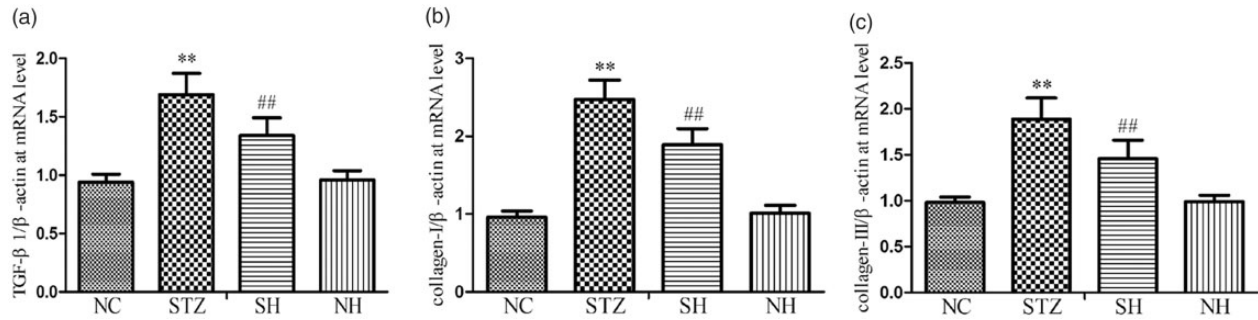


Figure 5. Effects of H₂S on (a) TGF-β1, (b) collagen-I, and (c) collagen-III mRNA expression in the diaphragm muscle. β-actin was used for normalization of mRNA expression levels. Values, mean ± SD; n = 8; **P < 0.01 vs. NC group; ##P < 0.01 vs. STZ group; NC: normal control group; STZ: streptozotocin group; SH: STZ + sodium hydrosulfide group; NH: NC + sodium hydrosulfide group.

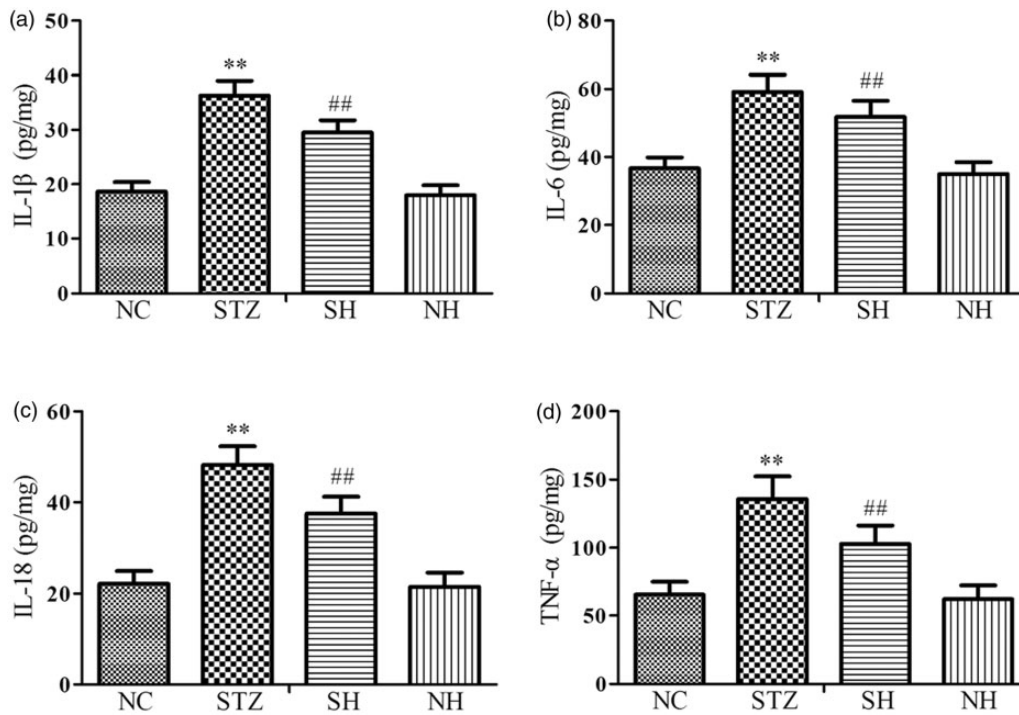


Figure 6. Effects of H₂S on inflammatory cytokines in the diaphragm muscle. (a) IL-1β, (b) IL-6, (c) IL-18, and (d) TNF-α. Values, mean ± SD; n = 8; **P < 0.01 vs. NC group; ##P < 0.01 vs. STZ group; NC: normal control group; STZ: streptozotocin group; SH: STZ + sodium hydrosulfide group; NH: NC + sodium hydrosulfide group.

extent of collagen deposition. Meanwhile, hydroxyproline is considered an important substrate for collagen formation, and, thus, hydroxyproline content is also used to assess the extent of fibrosis. The results of the present study show that the levels of stained collagen, hydroxyproline content, proinflammatory cytokines, and mRNA expression levels of TGF-β1 and collagen were notably raised in diabetic diaphragm muscle, which confirms that inflammatory reaction-mediated fibrosis of the diaphragm muscle is indeed present in diabetic rats.

Many pieces of evidence demonstrate that exogenous H₂S has anti-inflammatory and anti-fibrotic properties in diabetic animals,^{30,31} but the concrete molecular mechanism is still unclear. Recent research revealed that NLRP3 inflammasome activation induced the inflammatory process and tissue fibrosis.^{32,33} The NLRP3 inflammasome is a well-characterized multi-protein complex and comprises

mainly NLRP3 protein, Caspase-1, and ASC.³⁴ The activation of NLRP3 inflammasome leads to the maturation of proinflammatory cytokines, IL-18 and IL-1β. These proinflammatory mediators result in over-production of the pro-fibrotic cytokine, TGF-β1, which contributes to development of tissue fibrosis.³⁵ The current work shows that compared with the normal diaphragm, the expression levels of NLRP3 inflammasome-related proteins and the concentrations of IL-18 and IL-1β were raised in the diabetic rat diaphragm. Therefore, we inferred that the NLRP3 inflammasome might be the most important factor in regulation of diaphragm muscle inflammation in diabetic rats.

Recent research in a high glucose-induced cell model shows that H₂S mediates its anti-inflammatory properties by suppressing NLRP3 inflammasome activation.³⁶ Our previous study also revealed that H₂S alleviated the inflammatory reaction by inhibiting myocardial NLRP3

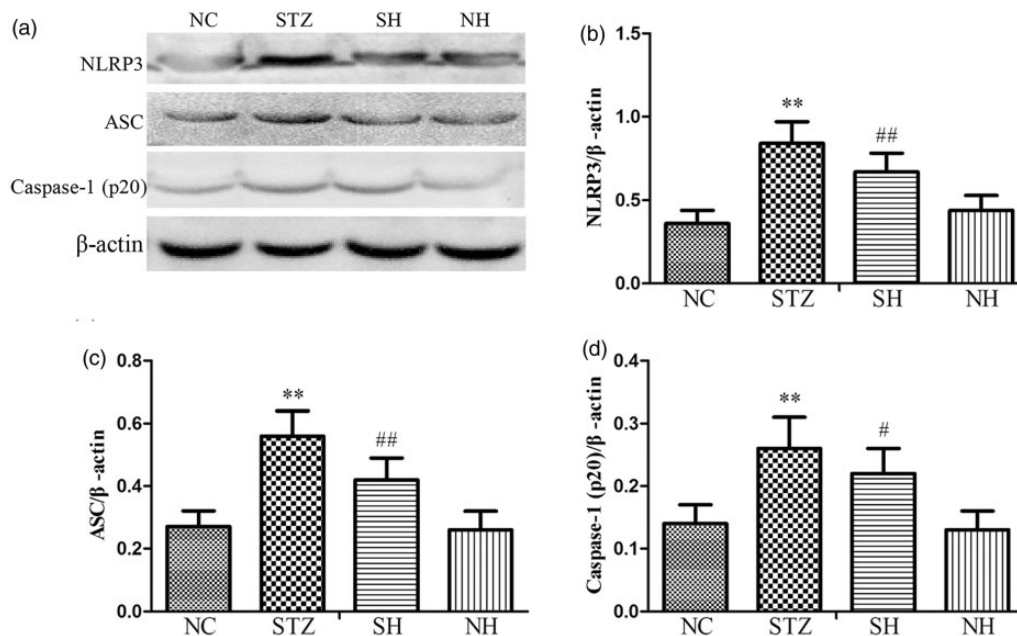


Figure 7. Effects of H₂S on NLRP3 inflammasome-related protein expression in the diaphragm muscle of each group. (a) Representative Western blotting results for NLRP3, ASC, and Caspase-1 (p20) in the diaphragm. (b) to (d) Quantitative analyses of NLRP3, ASC, and Caspase-1 (p20) proteins. β -Actin was utilized for normalization of protein expression levels. Values, mean \pm SD; $n = 8$; ** $P < 0.01$ vs. NC group; # $P < 0.05$, ## $P < 0.01$ vs. STZ group; NC: normal control group; STZ: streptozotocin group; SH: STZ + sodium hydrosulfide group; NH: NC + sodium hydrosulfide group.

inflammasome activation in STZ-induced diabetic animals.¹⁸ The findings of the current study show that on treatment with H₂S, the levels of inflammatory cytokines and NLRP3 inflammasome complex-related protein expression were noticeably decreased in diabetic diaphragm muscle, which reveals that H₂S alleviated diaphragmatic inflammation by suppressing activation of NLRP3 inflammasome in diabetic rats. On the other hand, Li *et al.* showed that H₂S ameliorated renal fibrosis through inhibition of TGF- β 1 signaling.³⁷ The current study also revealed that H₂S treatment effectively decreased levels of TGF- β 1 and expression of collagen in the diabetic diaphragm. Hence, our results further demonstrate that H₂S noticeably alleviates fibrosis of the diaphragm muscle by inhibiting NLRP3 inflammasome-mediated inflammatory reaction in diabetic rats.

In conclusion, results of this study, for the first time, demonstrate that H₂S attenuates STZ-induced diaphragm muscle fibrosis and strengthens diaphragmatic biomechanical properties in diabetes mellitus; the molecular mechanism may involve the alleviation of collagen deposition through suppression of NLRP3 inflammasome-mediated inflammatory reaction. This evidence suggests that therapeutic strategies aimed at inhibiting NLRP3 inflammasome-mediated fibrosis by use of exogenous H₂S might serve as efficient targeted therapy in diabetes mellitus.

AUTHORS' CONTRIBUTIONS: RY, QJ, YL, and SM carried out the experiments, and drafted and revised the manuscript.

DECLARATION OF CONFLICTING INTERESTS

The author(s) declared no potential conflicts of interest with respect to the research, authorship, and/or publication of this article.

FUNDING

The author(s) disclosed receipt of the following financial support for the research, authorship, and/or publication of this article: This work was supported by the Natural Science Research Project of the Education Commission of Anhui Province (No. KJ2018A0994); and the Training Programs of Innovation and Entrepreneurship for Undergraduates (Nos. 201810367054, 201910367038), China.

ORCID IDS

Rui Yang <https://orcid.org/0000-0003-3862-9069>
Qiang Jia <https://orcid.org/0000-0001-6689-5255>

REFERENCES

- Forbes JM, Cooper ME. Mechanisms of diabetic complications. *Physiol Rev* 2013;**93**:137–88
- Deshpande AD, Harris-Hayes M, Schootman M. Epidemiology of diabetes and diabetes-related complications. *Phys Ther* 2008;**88**:1254–64
- Farkhondeh T, Samarghandian S, Roshanravan B. Impact of chrysin on the molecular mechanisms underlying diabetic complications. *J Cell Physiol* 2019;**234**:17144–58
- Wanke T, Formanek D, Auinger M, Popp W, Zwick H, Irsigler K. Inspiratory muscle performance and pulmonary function changes in insulin-dependent diabetes mellitus. *Am Rev Respir Dis* 1991;**143**:97–100
- Allwood MA, Foster AJ, Arkell AM, Beaudoin MS, Snook LA, Romanova N, Murrant CL, Holloway GP, Wright DC, Simpson JA. Respiratory muscle weakness in the Zucker diabetic fatty rat. *Am J Physiol Regul Integr Comp Physiol* 2015;**309**:R780–7
- Jia Q, Yang R, Ma S, Liu X. Protective effect of genistein on diaphragm injury in diabetic rats. *Lat Am J Pharm* 2018;**37**:2145–53
- Fanning KM, Pfisterer B, Davis AT, Presley TD, Williams IM, Wasserman DH, Cline JM, Kavanagh K. Changes in microvascular density differentiate metabolic health outcomes in monkeys with prior

- radiation exposure and subsequent skeletal muscle ECM remodeling. *Am J Physiol Regul Integr Comp Physiol* 2017;**313**:R290–7
8. Lee H, Lim Y. Gamma-tocopherol ameliorates hyperglycemia-induced hepatic inflammation associated with NLRP3 inflammasome in alloxan-induced diabetic mice. *Nutr Res Pract* 2019;**13**:377–83
 9. Vince JE, Silke J. The intersection of cell death and inflammasome activation. *Cell Mol Life Sci* 2016;**73**:2349–67
 10. Sepehri Z, Kiani Z, Afshari M, Kohan F, Dalvand A, Ghavami S. Inflammasomes and type 2 diabetes: an updated systematic review. *Immunol Lett* 2017;**192**:97–103
 11. Wan Z, Fan Y, Liu X, Xue J, Han Z, Zhu C, Wang X. NLRP3 inflammasome promotes diabetes-induced endothelial inflammation and atherosclerosis. *Diabetes Metab Syndr Obes* 2019;**12**:1931–42
 12. Abderrazak A, El Hadri K, Bosc E, Blondeau B, Slimane MN, Buchele B, Simmet T, Couchie D, Rouis M. Inhibition of the inflammasome NLRP3 by arglabin attenuates inflammation, protects pancreatic β -cells from apoptosis, and prevents type 2 diabetes mellitus development in ApoE2K mice on a chronic high-fat diet. *J Pharmacol Exp Ther* 2016;**357**:487–94
 13. Wree A, McGeough MD, Inzaugarat ME, Eguchi A, Schuster S, Johnson CD, Pena CA, Geisler LJ, Papouchado BG, Hoffman HM, Feldstein AE. NLRP3 inflammasome driven liver injury and fibrosis: roles of IL-17 and TNF in mice. *Hepatology* 2018;**67**:736–49
 14. Seo JB, Choi YK, Woo HI, Jung YA, Lee S, Lee S, Park M, Lee IK, Jung GS, Park KG. Gemigliptin attenuates renal fibrosis through down-regulation of the NLRP3 inflammasome. *Diabetes Metab J* 2019;**43**:830–9
 15. Li Y, Li H, Liu S, Pan P, Su X, Tan H, Wu D, Zhang L, Song C, Dai M, Li Q, Mao Z, Long Y, Hu Y, Hu C. Pirfenidone ameliorates lipopolysaccharide-induced pulmonary inflammation and fibrosis by blocking NLRP3 inflammasome activation. *Mol Immunol* 2018;**99**:134–44
 16. Qiu H, Liu W, Lan T, Pan W, Chen X, Wu H, Xu D. Salvianolate reduces atrial fibrillation through suppressing atrial interstitial fibrosis by inhibiting TGF- β 1/Smad2/3 and TXNIP/NLRP3 inflammasome signaling pathways in post-MI rats. *Phytomedicine* 2018;**51**:255–65
 17. Li Z, Polhemus DJ, Lefter DJ. Evolution of hydrogen sulfide therapeutics to treat cardiovascular disease. *Circ Res* 2018;**123**:590–600
 18. Jia Q, Mehmood S, Liu X, Ma S, Yang R. Hydrogen sulfide mitigates myocardial inflammation by inhibiting nucleotide-binding oligomerization domain-like receptor protein 3 inflammasome activation in diabetic rats. *Exp Biol Med* 2020;**245**:221–30
 19. Lu Y, Gao L, Li L, Zhu Y, Wang Z, Shen H, Song K. Hydrogen sulfide alleviates peritoneal fibrosis via attenuating inflammation and TGF- β 1 synthesis. *Nephron* 2015;**131**:210–9
 20. Fusco L, Pitocco D, Longobardi A, Zaccardi F, Contu C, Pozzuto C, Basso S, Varone F, Ghirlanda G, Antonelli Incalzi R. Reduced respiratory muscle strength and endurance in type 2 diabetes mellitus. *Diabetes Metab Res Rev* 2012;**28**:370–5
 21. Smuder AJ, Falk DJ, Sollanek KJ, Nelson WB, Powers SK. Delivery of recombinant adeno-associated virus vectors to rat diaphragm muscle via direct intramuscular injection. *Hum Gene Ther Methods* 2013;**24**:364–71
 22. Szabo C. Roles of hydrogen sulfide in the pathogenesis of diabetes mellitus and its complications. *Antioxid Redox Signal* 2012;**17**:68–80
 23. Dorison A, Dussaule JC, Chatziantoniou C. The role of discoidin domain receptor 1 in inflammation, fibrosis and renal disease. *Nephron* 2017;**137**:212–20
 24. Jia Q, Yang R, Liu XF, Ma SF, Wang L. Genistein attenuates renal fibrosis in streptozotocin-induced diabetic rats. *Mol Med Rep* 2019;**19**:423–31
 25. Stewart AG, Thomas B, Koff J. TGF- β : Master regulator of inflammation and fibrosis. *Respirology* 2018;**23**:1096–7
 26. Li J, Wang Y, Ma M, Jiang S, Zhang X, Zhang Y, Yang X, Xu C, Tian G, Li Q, Wang Y, Zhu L, Nie H, Feng M, Xia Q, Gu J, Xu Q, Zhang Z. Autocrine CTHRC1 activates hepatic stellate cells and promotes liver fibrosis by activating TGF- β signaling. *EBioMedicine* 2019;**40**:43–55
 27. Annaldas S, Saifi MA, Khurana A, Godugu C. Nimbolide ameliorates unilateral ureteral obstruction-induced renal fibrosis by inhibition of TGF- β and EMT/slugg signalling. *Mol Immunol* 2019;**112**:247–55
 28. Wan Y, Xu L, Wang Y, Tuerdi N, Ye M, Qi R. Preventive effects of astragaloside IV and its active sapogenin cycloastragenol on cardiac fibrosis of mice by inhibiting the NLRP3 inflammasome. *Eur J Pharmacol* 2018;**833**:545–54
 29. Li J, Feng M, Sun R, Li Z, Hu L, Peng G, Xu X, Wang W, Cui F, Yue W, He J, Liu J. Andrographolide ameliorates bleomycin-induced pulmonary fibrosis by suppressing cell proliferation and myofibroblast differentiation of fibroblasts via the TGF- β 1-mediated smad-dependent and -independent pathways. *Toxicol Lett* 2020;**321**:103–13
 30. Yang R, Jia Q, Ma SF, Wang Y, Mehmood S, Chen Y. Exogenous H₂S mitigates myocardial fibrosis in diabetic rats through suppression of the canonical Wnt pathway. *Int J Mol Med* 2019;**44**:549–58
 31. Zhou X, Feng Y, Zhan Z, Chen J. Hydrogen sulfide alleviates diabetic nephropathy in a streptozotocin-induced diabetic rat model. *J Biol Chem* 2014;**289**:28827–34
 32. Mridha AR, Wree A, Robertson AAB, Yeh MM, Johnson CD, Van Rooyen DM, Haczeyni F, Teoh NC, Savard C, Ioannou GN, Masters SL, Schroder K, Cooper MA, Feldstein AE, Farrell GC. NLRP3 inflammasome blockade reduces liver inflammation and fibrosis in experimental NASH in mice. *J Hepatol* 2017;**66**:1037–46
 33. Wree A, Eguchi A, McGeough MD, Pena CA, Johnson CD, Canbay A, Hoffman HM, Feldstein AE. NLRP3 inflammasome activation results in hepatocyte pyroptosis, liver inflammation, and fibrosis in mice. *Hepatology* 2014;**59**:898–910
 34. Jo EK, Kim JK, Shin DM, Sasakawa C. Molecular mechanisms regulating NLRP3 inflammasome activation. *Cell Mol Immunol* 2016;**13**:148–59
 35. Li R, Lu K, Wang Y, Chen M, Zhang F, Shen H, Yao D, Gong K, Zhang Z. Triptolide attenuates pressure overload-induced myocardial remodeling in mice via the inhibition of NLRP3 inflammasome expression. *Biochem Biophys Res Commun* 2017;**485**:69–75
 36. Hu TX, Zhang NN, Ruan Y, Tan QY, Wang J. Hydrogen sulfide modulates high glucose-induced NLRP3 inflammasome activation in 3T3-L1 adipocytes. *Exp Ther Med* 2020;**19**:771–6
 37. Li Y, Li L, Zeng O, Liu JM, Yang J. H₂S improves renal fibrosis in STZ-induced diabetic rats by ameliorating TGF- β 1 expression. *Ren Fail* 2017;**39**:265–72

(Received February 9, 2020, Accepted May 11, 2020)